Molecular Biology of the Cell
Vol. 17, 3397–3408, August 2006

Targeting of Transmembrane Protein Shrew-1 to Adherens Junctions Is Controlled by Cytoplasmic Sorting Motifs

Viktor Jakob,* Alexander Schreiner,* Ritva Tikkanen,† and Anna Starzinski-Powitz*

*Institute of Cell Biology and Neuroscience, Johann-Wolfgang Goethe University of Frankfurt, D-60323 Frankfurt am Main, Germany; and †Institute of Biochemistry II, University Clinic of Frankfurt, D-60590 Frankfurt am Main, Germany

Submitted November 10, 2005; Revised May 3, 2006; Accepted May 5, 2006
Monitoring Editor: Jennifer Lippincott-Schwartz

We recently identified transmembrane protein shrew-1 and showed that it is able to target to adherens junctions in polarized epithelial cells. This suggested shrew-1 possesses specific basolateral sorting motifs, which we analyzed by mutational analysis. Systematic mutation of amino acids in putative sorting signals in the cytoplasmic domain of shrew-1 revealed three tyrosines and a dileucine motif necessary for basolateral sorting. Substitution of these amino acids leads to apical localization of shrew-1. By applying tannic acid to either the apical or basolateral part of polarized epithelial cells, thereby blocking vesicle fusion with the plasma membrane, we obtained evidence that the apically localized mutants were primarily targeted to the basolateral membrane and were then redistributed to the apical domain. Further support for a postendocytic sorting mechanism of shrew-1 was obtained by demonstrating that μ1B, a subunit of the epithelial cell-specific adaptor complex AP-1B, interacts with shrew-1. In conclusion, our data provide evidence for a scenario where shrew-1 is primarily delivered to the basolateral membrane by a so far unknown mechanism. Once there, adaptor protein complex AP-1B is involved in retaining shrew-1 at the basolateral membrane by postendocytic sorting mechanisms.

INTRODUCTION

Epithelial cells are highly polarized cells with an asymmetric distribution of proteins within the plasma membrane. Basically, the epithelial plasma membrane is divided into two major regions: the apical surface facing the extracellular space and the basolateral surface in contact with surrounding cells and the extracellular matrix (Rodriguez-Boulan and Nelson, 1989). In addition to distinct proteins, the lipid composition within these two membrane domains also differs significantly (Yeaman *et al*., 1999). To achieve the characteristic spatial expression patterns of proteins, epithelial cells display a variety of sorting mechanisms to ensure correct routing of proteins to the appropriate plasma membrane region. As shown for polarized epithelial Madin-Darby canine kidney (MDCK) cells, apical and basolateral transmembrane proteins are sorted into distinct vesicles that derive from the *trans*-Golgi network (TGN). These vesicles carry the proteins to the correct target plasma membrane domain (Ikonen and Simons, 1998; Matter, 2000; Mostov *et al*., 2000). Despite these observations and many additional studies, our understanding of how cells perform polarized sorting of proteins to different plasma membrane domains is still fragmentary. In particular, routing to the apical membrane is more poorly understood than basolateral targeting.

This article was published online ahead of print in *MBC in Press* (http://www.molbiolcell.org/cgi/doi/10.1091/mbc.E05–11–1034) on May 17, 2006.

Address correspondence to: Anna Starzinski-Powitz (starzinski-powitz@em.uni-frankfurt.de).

For basolateral sorting of transmembrane proteins, it has been established with several examples that targeting signals located in the cytoplasmic domains of proteins are required to mediate efficient sorting (Mellman, 1993; Ikonen and Simons, 1998). As opposed to other sorting information (e.g., GAT-2 GABA transporter; Brown *et al*., 2004), these so-called classical basolateral consensus sorting signals within the cytoplasmic domain of membrane proteins are tyrosine based (YXXΦ, where Y is tyrosine, X is any amino acid, and Φ is a bulky hydrophobic residue) and dileucine motifs (Bonifacino and Traub, 2003). In some cases, however, these sorting motifs are not necessarily colinear but apparently arise through folding (Orsel *et al*., 2000).

These short peptide motifs can be recognized by a variety of adaptor proteins (APs) peripherally associated with the cytosolic membrane. One family of APs includes AP-1 to AP-4 and Golgi-localized, γ ear-containing, ADP ribosylation factor-binding proteins (GGAs) (Kirchhausen, 1999; Bonifacino, 2004). Each of the AP family members exists as a heterotetramer consisting of two large (α, γ, δ, or ε, and $\beta_{1\text{-}4}$), one medium ($\mu_{1\text{-}4}$), and one small ($\sigma_{1\text{-}4}$) subunit, whereas GGAs are monomeric proteins (Hirst and Robinson, 1998; Bonifacino and Dell'Angelica, 1999; Bonifacino, 2004). In addition to the adaptor proteins, a set of accessory proteins is involved in the assembly of clathrin coats and vesicle budding (Pearse and Robinson, 1990; Kirchhausen, 2000; Slepnev and De Camilli, 2000). Several reports have indicated that the interaction between APs and their cargo may be regulated by phosphorylation and dephosphorylation events.

Our previous studies indicated that shrew-1, a type I transmembrane protein, is localized in the basolateral membrane of polarized epithelial MDCK cells and integrates

Table 1. Summary of all shrew-1 constructs used in this study

Name of mutant	Mutation	Distribution (%) AP	BL
Shrew-1 wild type	None	10 ± 4	90 ± 3
Shrew-1-TCD 30	Deletion 1–253	20 ± 4	80 ± 6
Shrew-1-NTD 5	Deletion 308–411	95 ± 3	5 ± 1
Shrew-1-L303A	Substitution L303A	65 ± 7.5	33 ± 5
Shrew-1-Y350A	Substitution Y350A	87 ± 6	13 ± 6
Shrew-1-Y368A	Substitution Y368A	89 ± 4	10 ± 5
Shrew-1-Y380A	Substitution Y380A	86 ± 4	12 ± 4
Shrew-1-L396A	Substitution L396A	79 ± 4	19 ± 3.5
Shrew-1-LI396/397HV	Substitution LI396/397HV	65 ± 4	35 ± 6
Shrew-1-K304A	Substitution K304A	33 ± 4	66 ± 3.5
Shrew-1-E359A	Substitution E359A	32 ± 8.5	67 ± 8

The percentage steady-state distribution between AP and BL membranes was measured (quantification of at least three independent experiments) for each shrew-1 variant using domain-selective biotinylation data.

specifically into E-cadherin-mediated adherens junctions (Bharti *et al.*, 2004). These results raised questions concerning the signals mediating this targeting and the protein(s) possibly involved.

Here, we show that the cytoplasmic domain of shrew-1 indeed contains basolateral sorting signals, which are functional in polarized epithelial cells. Systematic mutation of single amino acids in these putative sorting signals revealed three critical tyrosines and a dileucine motif within the cytoplasmic domain. These mutants localize apically instead of basolaterally and thus the mutated amino acids play an important role in shrew-1 targeting. By using tannic acid, we present evidence that the apically localized mutants were first targeted to the basolateral membrane and were then redistributed to the apical membrane. Furthermore, we demonstrate that μ1B, a subunit of adaptor protein AP-1B is important for retaining shrew-1 at the basolateral membrane, implying the involvement of postendocytic sorting machinery.

MATERIALS AND METHODS

Immunohistochemical Staining of Uterus Sections

Uterus tissue was collected from patients and stored in isopentane. Using Frigocut 2800 (Leica, Bensheim, Germany), 4-μm-thick cryostat sections were prepared and mounted on Superfrost Plus slides (Menzel-Glaeser, Braunschweig, Germany). The sections were fixed with ice-cold 4% paraformaldehyde for 30 min. After serum blocking (10% fetal calf serum [FCS] in phosphate-buffered saline [PBS]) incubation with the primary antibodies was performed for 1–2 h. Shrew-1 staining was achieved using rat anti-shrew-1 polyclonal antibody (MorphoSys, Munich, Germany) in an appropriate dilution. β-catenin and E-cadherin were stained with rabbit anti-β-catenin or anti-E-cadherin polyclonal antibodies (Santa Cruz Biotechnology, Santa Cruz, CA). To visualize the proteins, fluorescent-conjugated antibodies derived from goat Alexa-Fluor 488 anti-mouse and Alexa-Fluor 594 anti-rabbit (Invitrogen, Carlsbad, CA) were used. The nuclei were counterstained with ToPro-3. The sections were analyzed using confocal microscope LSM 510 (Carl Zeiss, Jena, Germany). x,z and three-dimensional (3D) reconstructions were generated using Imaris 4.0.4 software (Bitplane, Zurich, Switzerland).

Construction of cDNAs Encoding Shrew-1-GFP Mutants

pEGFP-N3-Shrew-1 (Bharti *et al.*, 2004) (Clontech, Mountain View, CA) was used as a source of cDNA encoding human shrew-1 (GenBank accession no. AY282806). The deletion mutants were derived by PCR using sets of primers obtained from Sigma-Genosys (Cambridge, United Kingdom). The newly introduced restriction sites HindIII and Acc65I were used to reclone the mutant shrew-1 cDNA into pEGFP-N3 vector. A GeneTailor site-directed mutagenesis kit (Invitrogen, Karlsruhe, Germany) was used to introduce substitutions within the shrew-1 cDNA. The different shrew-1 constructs generated are listed in Table 1. All constructs were subsequently sequenced to verify the intended mutation. DNA sequencing was performed by GENterprice (Mainz, Germany).

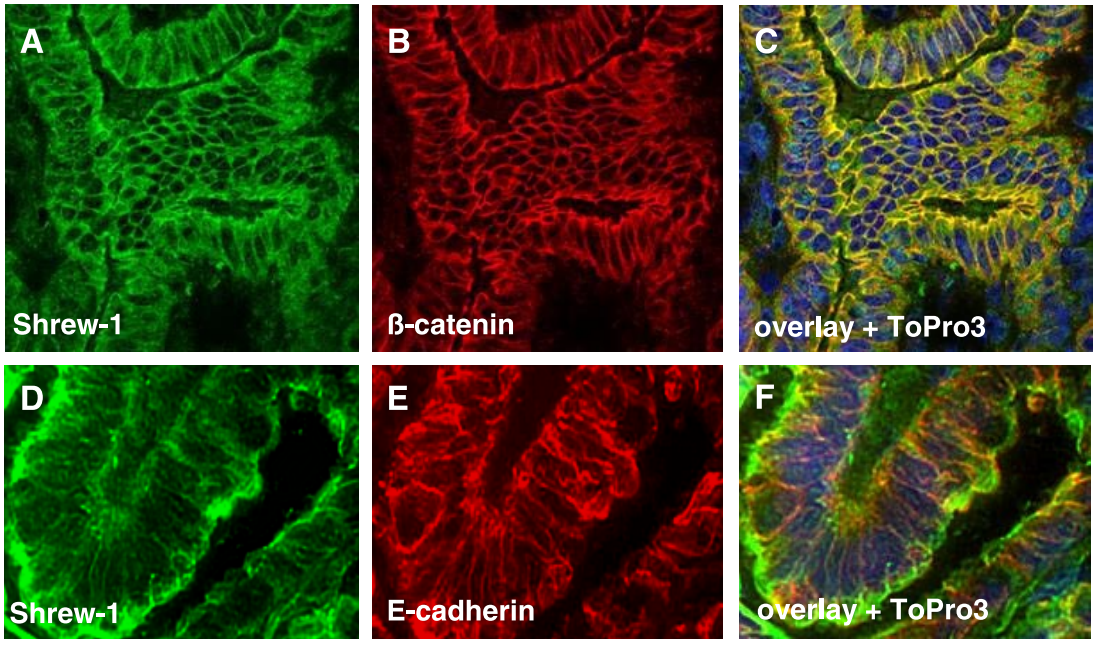

Figure 1. Localization of shrew-1 in human uterus tissue. Immunofluorescence staining for shrew-1, β-catenin, and E-cadherin in cryosectioned uterus. (A and D) Shrew-1 staining. (B) β-catenin staining. (E) E-cadherin staining. (C and F) Merged pictures with counterstained nuclei.

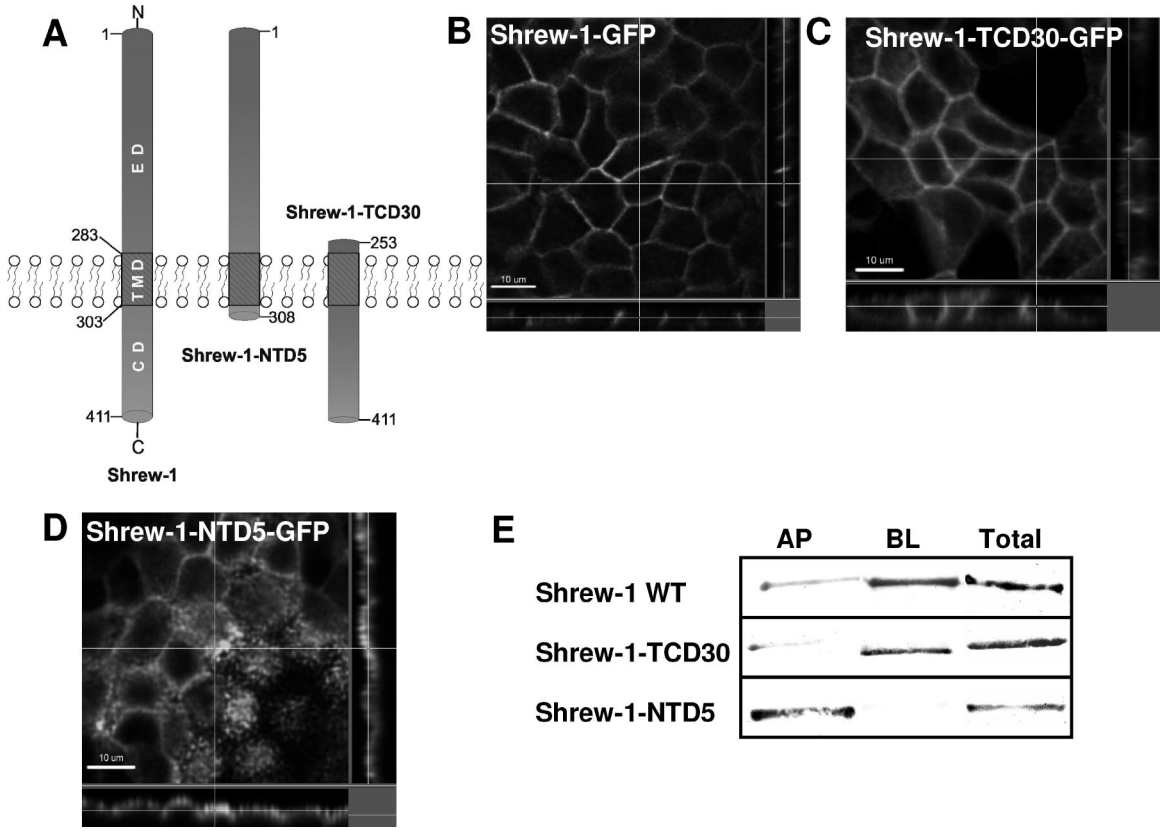

Figure 2. Steady-state distribution of GFP-tagged shrew-1 mutants between the apical and basolateral membranes in polarized MDCK cells. (A) Diagram represents the structure of wild-type shrew-1 and the deletion mutant constructs shrew-1-TCD30 and shrew-1-NTD5, drawn to scale to show the number of amino acid residues remaining after deletion of either the ectodomain (ED) or cytoplasmic domain (CD). (B–D) Localization of shrew-1 mutants at the cell surface. MDCK cells were stably transfected with human wild-type or mutant shrew-1; the cells were plated on Transwell filters and grown to confluent, polarized cell layers. The cells were then fixed and analyzed by confocal microscopy. z,x and z,y reconstructions are shown for each shrew-1 variant. Basolateral cell surface localization is seen with wild-type shrew-1-GFP (B) and shrew-1-TCD30-GFP mutant (C), whereas the mutant shrew-1-NTD5-GFP is localized apically (D). (E) Biotinylation results to measure the amount of apically and basolaterally localized shrew-1 protein. Polarized MDCK cells were biotinylated from either the basolateral or apical side. Cell lysates were incubated with Neutravidin beads. Biotinylated proteins were eluted from the beads, analyzed by SDS-PAGE, and immunostained using the antibody against GFP. Densitometry quantification results of shrew-1 percentages found at the apical (AP) or basolateral (BL) side in polarized MDCK cells are also listed in Table 1.

Cell Culture

MDCK, porcine kidney (LLC-PK1), and human mammary carcinoma (MCF-7) cells were cultured in DMEM (Invitrogen) supplemented with 10% FCS (PAA Laboratories, Coelbe, Germany), 1% penicillin, and 100 U/ml streptomycin (Invitrogen) 37°C with 5% CO_2.

Cell Transfection

To obtain cell lines stably expressing wild-type or mutant shrew-1-GFP, MDCK and LLC-PK1 cells were grown on 10-cm plates until 40% confluent and transfected with wild-type or mutant pEGFP-shrew-1 applying magnet-assisted transfection (MaTra) (IBA, Goettingen, Germany). Stable cell lines were selected by adding the eukaryotic selection marker G418 (Invitrogen) at a final concentration of 5 mg/ml 48 h after transfection. This concentration of G418 was maintained until single colonies formed. Twenty to 25 colonies were isolated, expanded, and grown in the presence of 0.5 mg of G418 per milliliter of medium. Double-transfected LLC-PK1 cells were obtained as described for LLC-PK1 cells. Additionally, pCB6-μ1B-HA or pCB6-μ1A-HA were cotransfected. The expression of μ1B-HA was then determined in vivo and in vitro using a monoclonal anti-hemagglutinin (HA) antibody (Covance, Berkeley, CA) at an appropriate dilution. For colocalization studies of shrew-1 with endocytic markers, MCF-7 cells were transfected with pEGFP-shrew-1 plasmid using MaTra. Cells were fixed after 24 h, and for endosome staining polyclonal anti-rab5 and anti-rab11 antibodies (Santa Cruz Biotechnology) and secondary anti-rabbit Alexa-Fluor 594 were used. The cells were then processed for immunofluorescence.

Confocal Microscopic Identification of Site of Expression of Shrew-1-GFP Mutants

MDCK and LLC-PK1 cells expressing wild-type or mutant shrew-1-GFP were grown for at least 5 d after becoming confluent on Transwell filter inserts (Corning Glassworks, Corning, NY). Staining of tight junctions was achieved using polyclonal rabbit anti-occludin antibody (Zymed, Invitrogen, Karlsruhe, Germany) and subsequent incubation with anti-rabbit Alexa-Fluor 594 antibody. Confocal images were acquired using Leica TCS NT and Leica TCS SP5 scanner (Leica). x,z and 3D reconstructions were generated using Imaris 4.5.1 software (Bitplane, Zurich).

Analysis of Surface Shrew-1-GFP Content by Surface-specific Biotinylation

MDCK cells stably expressing wild-type or mutant shrew-1-GFP were grown on Transwell inserts for at least 7 d in six-well plates. Cell monolayers were biotinylated with EZ-Link Sulfo-NHS-SS-Biotin (Pierce, Perbio Science, Bonn, Germany) that was added from either the apical or basal side. After washing, cells were lysed, and the membrane was solubilized using 10 mM Tris, pH 8.0, 150 mM NaCl, 1% Triton X-100, and 5 mM EDTA. Cell lysates were clarified by centrifugation (15,000 $\times$ *g*; 10 min). Samples containing 10% of supernatant were analyzed by SDS-PAGE to estimate the total amount of shrew-1-GFP in the supernatant. To isolate biotinylated proteins, the rest of each supernatant was incubated with 50 μl of Neutravidin beads (Pierce, Perbio Science) in a total volume of 500 μl of lysis buffer for 1 h at 4°C with continuous rotation. The beads were washed three times with lysis buffer, and the proteins were eluted from the beads by incubation in 25 μl of Roti-Load1 sample buffer (Carl

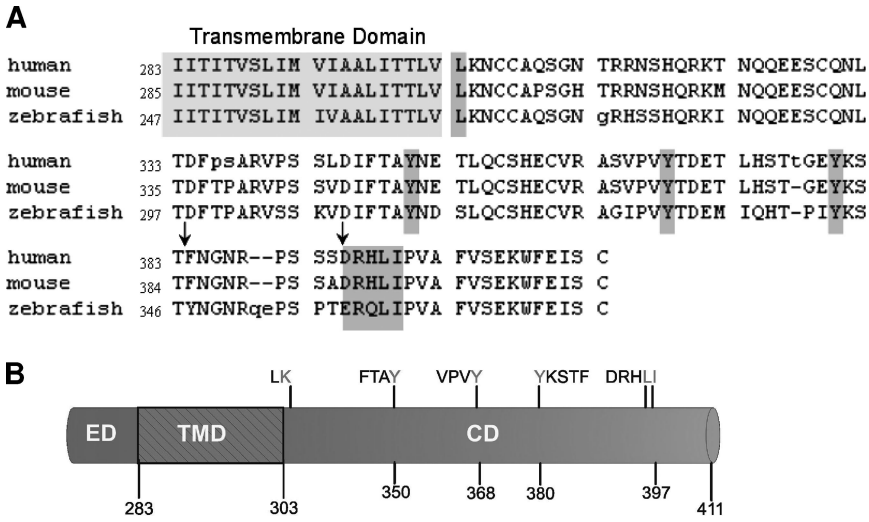

Figure 3. (A) Schematic representation of shrew-1 CD with predicted signals thought to be sufficient for basolateral targeting. The numbers define sites of putative tyrosine based signals (Y350, Y368, and Y380) as well as leucine motifs (L303 and LI396/397) within the CD. (B) The single leucine, tyrosine-based signals and an acidic dileucine motif within the CD of shrew-1, proposed to have an effect on sorting, are conserved across species. The amino acid composition of human shrew-1 CD is 93% identical and 95% similar to the murine shrew-1 CD and 79% identical and 87% similar to the zebrafish shrew-1 CD. The arrows mark some important deviations between the amino acid sequences (see *Discussion*).

Roth, Karlsruhe, Germany) 5 min at 95°C, separated by SDS-PAGE, and analyzed by Western blot using monoclonal anti-green fluorescent protein (GFP) antibody (Roche Diagnostics, Mannheim, Germany) and as secondary antibody an anti-mouse IgG conjugated to alkaline phosphatase (ALP) (Jackson ImmunoResearch, Dianova, Hamburg, Germany). Immunoblots were quantified by densitometry and the amount of surface shrew-1-GFP was normalized to the total labeled shrew-1-GFP using Scion image software (Scion, Frederick, MD). The representative immunoblots are shown in Figures 2 and 4.

Coimmunoprecipitation

For coimmunoprecipitations, a 3-cm dish of cells was incubated in 200 μl of lysis buffer (10 mM Tris, pH 8.0, 150 mM NaCl, 5 mM EDTA, 1% Triton X-100, and 60 mM octyl-β-D-glucopyranoside) supplemented with protease inhibitor mixture (Complete, protease inhibitor cocktail; Roche Diagnostics) at 4°C for 30 min. Insoluble material was removed by centrifugation at 10,000 $\times$ *g* at 4°C for 10 min. Lysate was incubated with 0.5 μg of anti-HA monoclonal antibody (mAb) (Covance) and immobilized protein G-agarose beads at 4°C for 4 h. Beads were then washed four times with cold lysis buffer. SDS-PAGE sample buffer was added to the immunoprecipitates, and samples were heated to 95°C for 5 min, separated by SDS-PAGE, and analyzed by Western blot using monoclonal anti-GFP antibody (Roche Diagnostics). Staining was achieved using anti-mouse IgG conjugated to ALP.

Tannic Acid Treatment

Tannic acid treatment was performed as described previously (Polishchuk *et al*., 2004). Briefly, stably expressing wild-type or mutant shrew-1-GFP MDCK cells were grown on Transwell inserts for at least 7 d to obtain proper tight junction development and electrically tight monolayers (>100 Ω cm^{-2}). Cells were then incubated at 20°C for 4 h to accumulate shrew-1-GFP within the Golgi apparatus. A temperature shift to 37°C was performed to release protein from the Golgi. During the shift from 20 to 37°C, 0.5% (wt/vol) tannic acid (Sigma-Aldrich, Munich, Germany) was added either to apical or basal growth medium. Tannic acid-treated cells were then fixed after 45 min and examined by confocal microscopy.

Antibody Uptake

MDCK and LLC-PK1 cells stably expressing wild-type or mutant shrew-1-GFP were grown on Transwell inserts for 7 d. The basal chamber was washed with PBS and refilled with DMEM medium supplemented with shrew-1 monoclonal antibodies (nanoTools, Tenningen, Germany) in a concentration of 10 μg/ml. The cells were incubated at 4°C for 30 min and either fixed or the medium was changed and the cells were incubated at 37°C for 60 min and then fixed. The cells were incubated in blocking buffer (10% FCS in PBS) for 1 h and stained with secondary anti-mouse Alexa-Fluor 594 antibodies (Molecular Probes) for an additional hour. The cells were then washed and processed for immunofluorescence.

RESULTS

Localization of Endogenous Shrew-1

Previous studies of shrew-1 ectopically expressed in epithelial MDCK and MCF7 cell lines showed that it is able to target to adherens junctions, where it colocalizes and coimmunoprecipitates with the E-cadherin–catenin complex (Bharti *et al*., 2004). To show that the ectopic expression of shrew-1 reflects the expression in vivo, endogenous shrew-1 localization was analyzed in frozen sections of human endometrium using polyclonal rat shrew-1 antibodies (Figure 1, A and D, green fluorescence). The results suggested that shrew-1 also localizes at the plasma membrane in tissue. To substantiate this interpretation more in detail, the sections were costained with antibody directed against either E-cadherin (Figure 1E, red fluorescence), the transmembrane protein characterizing adherens junctions of epithelial cells, or with antibody against β-catenin (Figure 1B, red fluorescence), which is a cadherin-binding protein and thus also shows plasma membrane localization. The merged pictures of shrew-1 with either E-cadherin or β-catenin as revealed by confocal microscopy (merged pictures in Figure 1, C and F) clearly indicate plasma membrane localization of shrew-1 in vivo. Therefore, these data imply that the previously reported targeting of shrew-1 to adherens junctions in polarized epithelial cells is indeed reflected by the in vivo situation in this cell type.

Mapping the Protein Region Responsible for Basolateral Sorting of Shrew-1

To define the steady-state distribution of shrew-1 in the plasma membrane of polarized epithelial cells more in detail, we used MDCK cells. For this purpose, MDCK cells were generated that stably express C-terminally GFP-tagged shrew-1. For the experiments performed throughout this article, it was important to demonstrate that the MDCK cells stably expressing shrew-1 behave as shown previously. Here, shrew-1 was found in adherens junctions of polarized MDCK cells, irrespective of whether it was fused to GFP or a 10-amino acid-long birch profilin tag, indicating that none of the tags disturbed the physiological targeting described in this article (Figure 1). Moreover, it has been also demonstrated that shrew-1 is an integral membrane protein and can be labeled with biotin by surface biotinylation of cells (Bharti *et al*., 2004).

Based on these findings, MDCK cells stably expressing shrew-1-GFP, here wild-type shrew-1, were plated on Transwell filters and grown for 7 d to ensure proper polarization. The spatial distribution of shrew-1-GFP between apical and basolateral membranes was visualized by confocal micros-

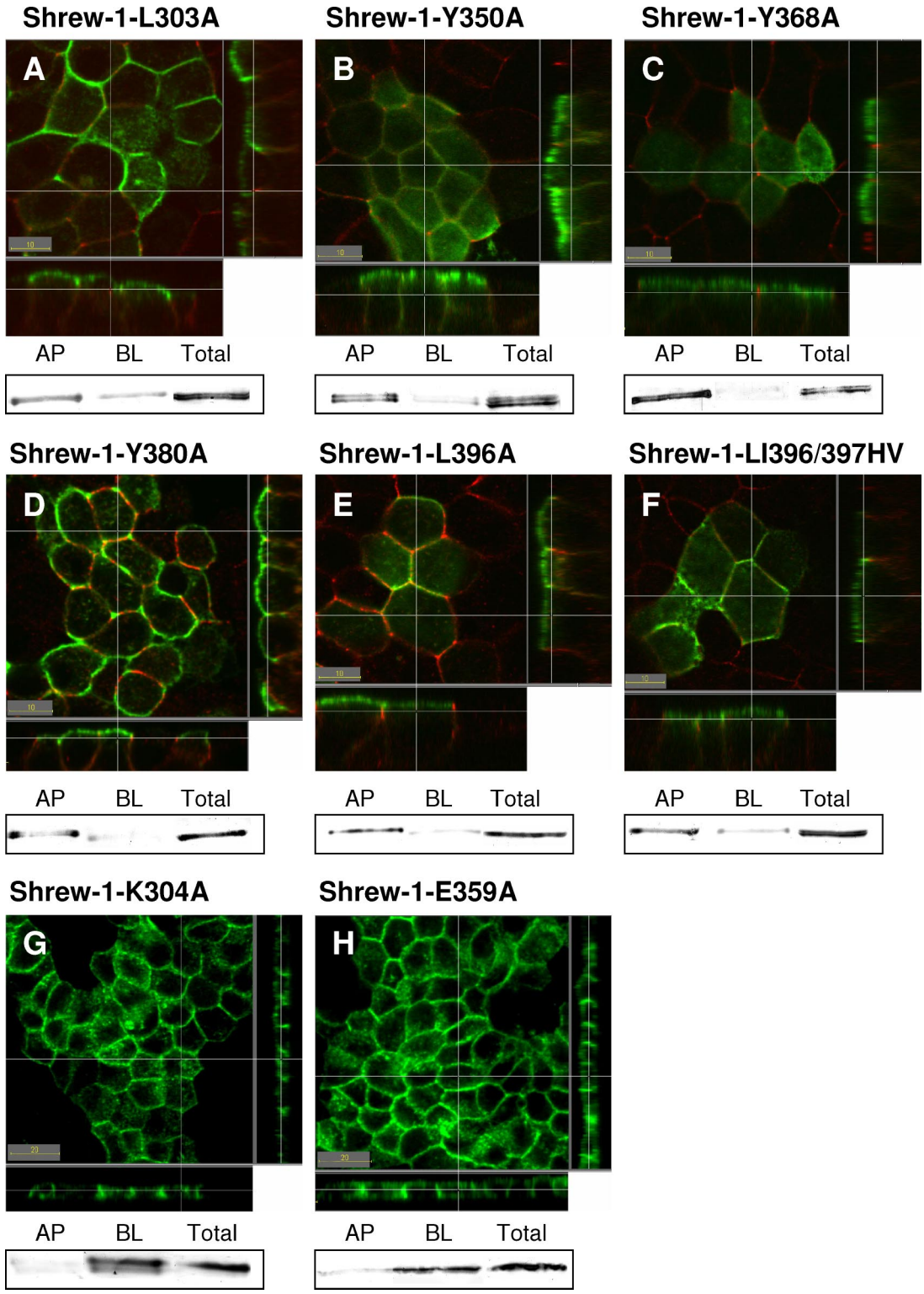

Figure 4. Cell surface localization of shrew-1 point mutants in polarized MDCK cells. (A–H) MDCK cells were stably transfected with shrew-1-GFP mutants, grown on Transwell filters until polarization, fixed, and analyzed by confocal microscopy. (A–F) For better differentiation between the AP and BL membrane domains, we visualized tight junctions using anti-occludin antibody (red staining). Along with the biotinylation data also shown for each mutant, apical distribution could be confirmed for shrew-1 mutants A-F. (G and H) Mutations introduced within the CD of shrew-1 that do not alter the distribution. The point mutants shrew-1-K305A (G) and shrew-1-E360A (H) are mainly localized basolaterally.

copy and by performing optical sectioning. This analysis once more confirmed that shrew-1-GFP wild type is sorted to the basolateral side of the cell and hardly any apical localization could be detected (Figure 2B). To support this

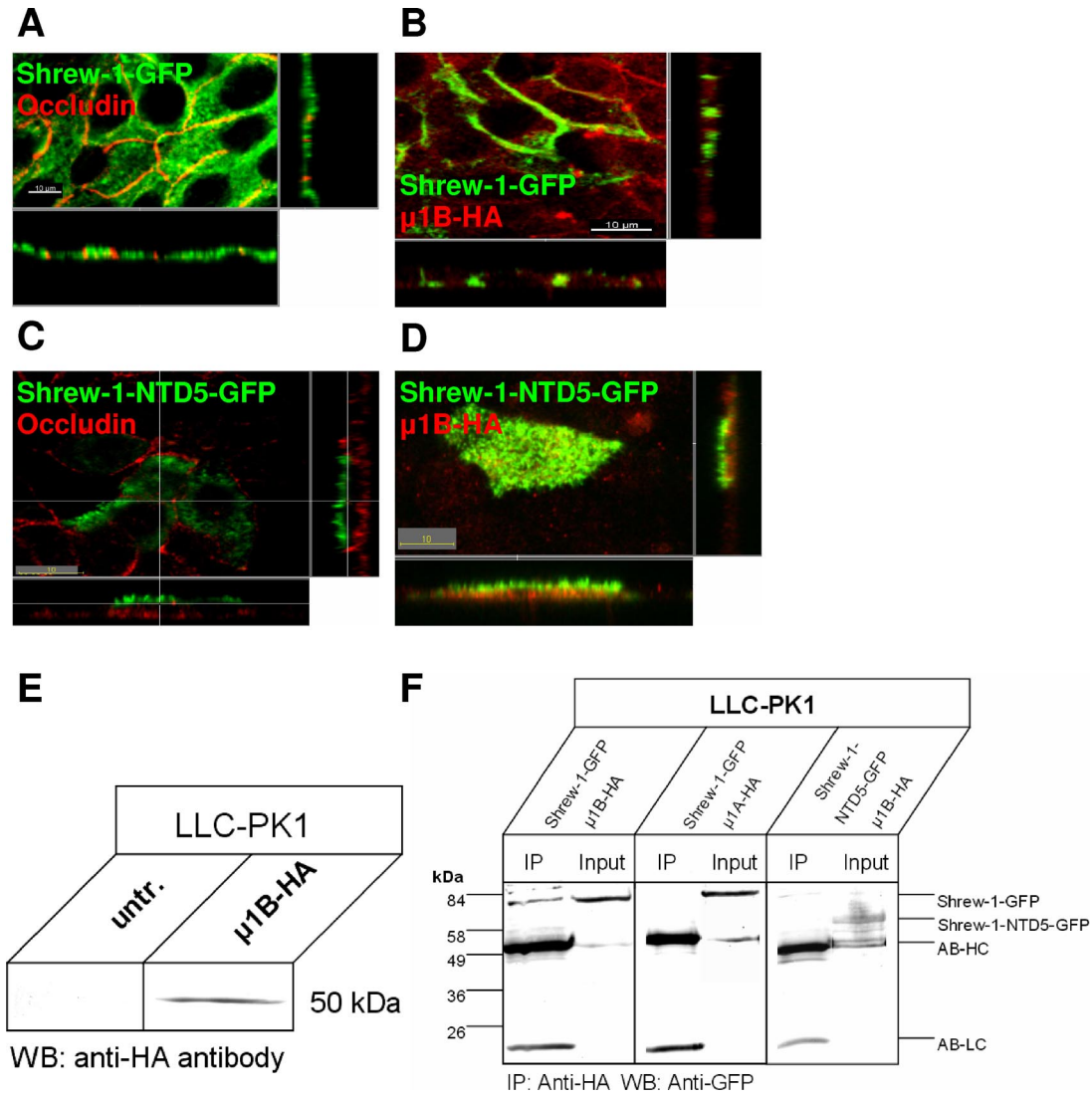

Figure 5. Localization of shrew-1 variants in wild-type LLC-PK1 cells and after ectopic expression of µ1B-HA. (A–D) LLC-PK1 cells were transiently transfected with wild-type or mutant shrew-1, allowed to grow to confluence on filters, fixed, and analyzed by confocal microscopy. (A–D) LLC-PK1 cells sort wild-type shrew-1-GFP as well as deletion mutant shrew-1-NTD5-GFP to the apical membrane. Tight junctions were visualized with anti-occludin antibody (red). Distribution of wild-type shrew-1 (B) to the basolateral membrane was restored after LLC-PK1 cells were transfected with HA-tagged µ1B subunit, whereas localization of shrew-1-NTD5-GFP (D) lacking the CD could not be restored after transfection with µ1B. Expression of µ1B in LLC-PK1 cells was confirmed using an HA-specific antibody. (E) Expression of µ1B-HA after transfection analyzed by Western blotting using an anti-HA antibody. (F) Lysates from LLC-PK1 cells expressing shrew-1-GFP and µ1B-HA, shrew-1-GFP and µ1A-HA, or shrew-1-NTD5-GFP and µ1B-HA were immunoprecipitated with anti-HA antibody. Precipitated proteins were blotted with anti-GFP antibody. Shrew-1 only coprecipitates in cells expressing µ1B subunit. Shrew-1 is not immunoprecipitated in cells expressing µ1A. µ1B did not coprecipitate with the mutant shrew-1-NTD5-GFP.

observation with a biochemical method, surface selective biotinylation was performed. This allows quantitative comparisons of the amounts of shrew-1-GFP in apical and basolateral membrane domains. Cell monolayers were surface biotinylated from either the apical or basolateral side. Biotinylated proteins were purified with Neutravidin beads and analyzed by Western blots stained with GFP antibodies to visualize shrew-1-GFP. Quantification of the Western blots (Figure 2E) revealed that ~90% of the total surface shrew-1-GFP was present in the basolateral domain and ~10% in the apical domain of the polarized MDCK cells.

Obviously, shrew-1 is targeted specifically to the basolateral domain of the plasma membrane of polarized epithelial cells. This raised questions about the intramolecular localization and peptide sequence of the signals required for the intracellular sorting of shrew-1, which we investigated using mutant shrew-1 constructs. First, shrew-1 deletion mutants were generated containing variable deletions of either the cytoplasmic domain (shrew-1-NTD5) or the ectodomain (shrew-1-CPD30) (Figure 2A). As with wild-type shrew-1, the mutants were fused to GFP and stably expressed in MDCK cells that were polarized before confocal laser scanning microscopy analysis. As shown in Figure 2C, almost complete truncation of the ectodomain still resulted in a subcellular localization almost comparable with the wild-type pattern (Figure 2B). However, if most of the cytoplasmic domain was deleted, shrew-1 localized predominantly to the apical membrane part of the polarized cells (Figure 2D).

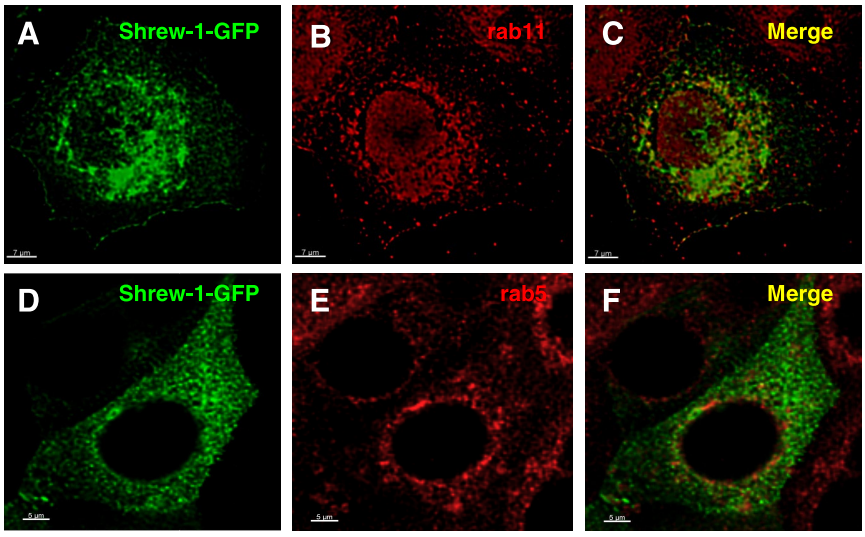

Figure 6. Colocalization analysis of shrew-1-GFP with rab GTPases rab5 and rab11. (A–F) MCF-7 cells were transfected with shrew-1-GFP, fixed 24 h later, and stained with anti-rab5 or anti-rab11 antibodies. Bound anti-rab5 and anti-rab11 antibodies were detected using Alexa-Fluor 594 anti-rabbit antibody. Shrew-1-GFP colocalized with rab11 (C) and displayed no colocalization with rab5 (F).

Microscopy analysis was confirmed by using a surface selective biotinylation assay of either the apical or basolateral side of the polarized MDCK cells (Figure 2E). Quantification of the biotinylated protein isolated from the basolateral and apical side of shrew-1-TCD30 expressing MDCK cells revealed a distribution of 80% of shrew-1 protein at the basolateral and 20% at the apical side. Biochemical analysis of shrew-1-NTD5 in polarized MDCK cells showed almost the reverse distribution, namely, 95% of the protein at the apical side and only 5% in the basolateral region.

Altogether, these findings imply that the cytoplasmic tail of shrew-1 is of fundamental importance for sorting and that the amino acid region between 303 and 411 of the shrew-1 protein sequence should contain essential targeting signals. In line with this, the ectodomain should not contain any basolateral targeting signal because deletion of this domain does not affect basolateral sorting. At this point, we can, however, not fully exclude that the ectodomain of shrew-1 contains some hidden apical sorting signals.

Basolateral Sorting Motifs in Shrew-1

Because we know that the cytoplasmic domain must harbor the signal for basolateral targeting, we focused on this domain to identify specific signals. First, we screened the cytoplasmic domain sequence for potential basolateral sorting signals that might resemble known signals. This analysis revealed five putative signals (Figure 3). Shrew-1 contains a single leucine at position 303, correlating with a basolateral sorting signal described in transmembrane protein CD147 (Deora *et al.*, 2004). In addition, three putative tyrosine-based signals at positions 350, 368, and 380 resemble, but do not perfectly match, consensus basolateral sorting motifs YXXΦ and YXXXΦ deduced from the analysis of several membrane proteins (Ikonen and Simons, 1998; Nelson and Yeaman, 2001; Mostov *et al.*, 2003; Nelson, 2003; Deora *et al.*, 2004; see *Introduction*). Finally, we detected an acidic dileucine motif at position 396/397, which was also described as a basolateral signal for several proteins (Ikonen and Simons, 1998; Nelson and Yeaman, 2001; Mostov *et al.*, 2003; Nelson, 2003; Deora *et al.*, 2004).

The mutants produced are shown in Figure 3 and Table 1. In addition to those already mentioned above, lysine 304 was mutated to alanine. This was intended as an internal control because a comparable mutation in CD147 had no effect on its localization (Deora *et al.*, 2004). Finally, glutamate at position 359 was changed to alanine, again as a

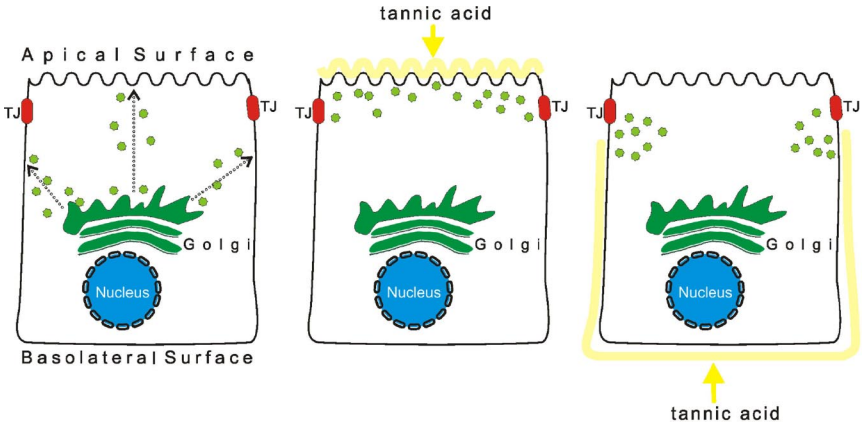

Figure 7. Schematic representation of experimental setup for testing trafficking of apically localized shrew-1 variants to apical plasma membrane in polarized MDCK cells. On leaving the TGN, shrew-1-NTD5-GFP could either be sorted directly to the apical membrane, or indirectly, i.e., initially destined for the basolateral membrane, and then resorted to the apical membrane. Administration of tannic acid (which selectively inhibits vesicle fusion to plasma membrane) to either the apical or basolateral side of polarized MDCK cells should help unravel whether the basolateral membrane is the first destination on the way to the apical membrane. If after application of tannic acid to the apical side, shrew-1-NTD-5 was found either on the basolateral plasma membrane and/or it accumulated in vesicles close to the tight junctions (TJ), this would indicate that shrew-1-NTD5-GFP can be delivered to the basolateral membrane. If after application of tannic acid to the basolateral side, shrew-1-NTD5 occurred on the apical membrane or no membrane localization was seen, only accumulation of vesicles adjacent to the basolateral membrane, this would suggest the direct route of shrew-1-NTD5-GFP to the apical membrane or the need for basolateral membrane participation.

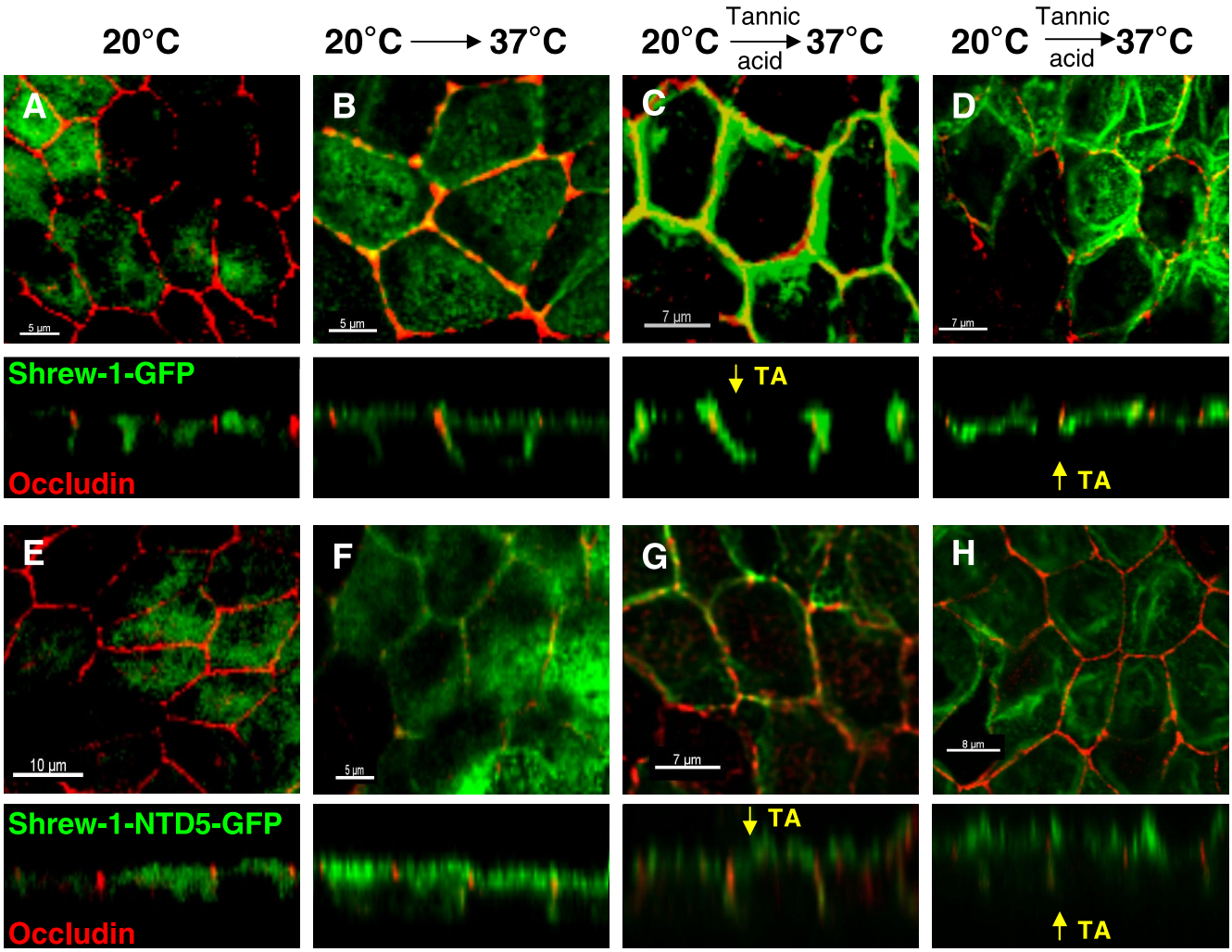

Figure 8. Domain-selective tannic acid administration to polarized MDCK cells stably expressing either wild-type shrew-1-GFP or mutant shrew-1-NTD5-GFP lacking the cytoplasmic domain. MDCK cells were plated on Transwell filters and grown for 7 d to complete polarization. On the day of treatment, the cells were incubated at 20°C for 4 h to accumulate proteins in the Golgi (A and E) and then shifted to 37°C to allow protein release (B and F), when tannic (TA) acid was added either apically or basolaterally. The cells were fixed after 45 min of incubation, stained with anti-occludin antibody and analyzed by confocal microscopy. After apical administration, shrew-1-GFP is still localized at the basolateral membrane (C), shrew-1-NTD5-GFP is localized basolaterally and accumulates close to the apex of the lateral membrane was observed (G). (D and H) basolateral administration of TA caused shrew-1-GFP and shrew-1-NTD5-GFP to accumulate in vesicles near the zone of tight junctions. No apical localization in the case of shrew-1-NTD5-GFP was detected (H).

control to exclude the possibility that the effect on sorting might be caused by mutation of any amino acid in the cytoplasmic domain.

As with the deletion mutants, the steady-state distribution of shrew-1 point mutants stably expressed in MDCK was examined by confocal microscopy and confirmed by surface selective biotinylation. For better distinction between apical and basolateral membranes in optical sections and to confirm polarization, we stained tight junctions using anti-occludin antibody (Figure 4, A–F, red staining).

The experiments revealed that the mutations L303A, Y350A, Y368A, Y380A, L396A, and LI396/397HV within the cytoplasmic domain of shrew-1 misdirected the protein to the apical membrane (Figure 4, A–F). Surface biotinylation of cell monolayers from either the apical or basolateral side confirmed the microscopy observation. Indeed, estimation of surface shrew-1 protein by Western blot analysis indicated that, depending on the mutant, between 65 and 90% of the total surface shrew-1 was present in the apical membrane and ~10–35% in the basolateral membrane of the polarized MDCK cells (Figure 4, A–F, and Table 1).

The strongest missorting of shrew-1 to the apical membrane was caused by mutation of the tyrosine-based targeting signals. Interestingly, of these Y368A showed the strongest apical targeting (Figure 4C). The L396A and LI396/397HV mutants also displayed apical localization. It seems, however, that the misrouting of the double mutant LI396/397HV (Figure 4F and Table 1; 65% apical, 35% basolateral) was less than that of the single mutant L396A (Figure 4E and Table 1; 79% apical, 19% basolateral) but comparable with that of L303A (Figure 4A and Table 1; 65% apical, 35% basolateral).

As expected, the exchange of lysine at position 304 to alanine did not alter the membrane localization of shrew-1 with respect to wild type (Figure 4G), nor did substitution E359A have any visible effect (Figure 4H). They were mainly

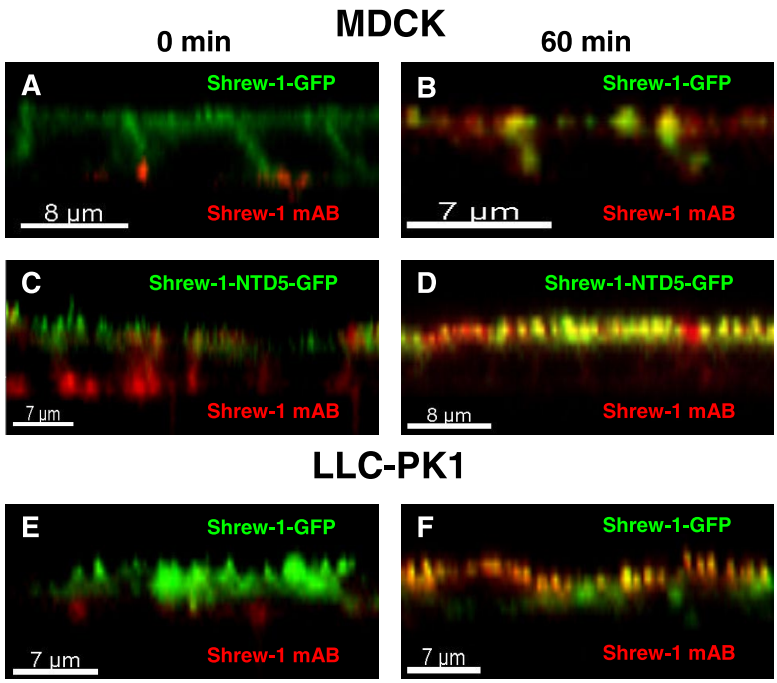

Figure 9. Transcytosis of wild-type and mutant shrew-1-GFP in polarized MDCK and LLC-PK1 cells. Cells stably expressing shrew-1-GFP or shrew-1-NTD5-GFP were grown on filters for 7 d until polarization. Anti-shrew-1 mAb was added to the basal chamber. After incubation for 30 min at 4°C the cells were either fixed (0 min) (A, C, and E) or, after removal of unbound antibody, incubated at 37°C for 60 min (B, D, and F) to allow the antibody to internalize. After fixation of the cells, bound anti-shrew-1 antibody was detected using Alexa-Fluor 594 anti-mouse antibody. Shrew-1-GFP and shrew-1-NTD5-GFP are found at the basolateral cell surface in MDCK cells (A and C). Subsequently, MDCK cells sorted mutant shrew-1-NTD5-GFP to the apical surface. (F) In LLC-PK1 cells, the wild-type shrew-1-GFP and the antibody were transported from the basolateral to apical part of the cells (E and F).

found, both microscopically and biochemically, in the basolateral part of the cell membrane (Figure 4, G and H, and Table 1).

These data demonstrate that the tyrosines and specific leucines within the cytoplasmic domain of shrew-1 are involved in the control of trafficking and positioning of the protein: mutation of these amino acids leads to an alternative distribution of shrew-1 in the polarized cell membrane of epithelial cells.

Expression of Wild-Type and Mutant Shrew-1 in LLC-PK1 Cells

An alternative epithelial cell type, LLC-PK1, was used to examine possible discrepancies in sorting of wild-type and mutant shrew-1. It is known that LLC-PK1 cells in contrast to MDCK cells exhibit different protein sorting of, for example, H^+,K^+-ATPase β-subunit (Duffield *et al.*, 2004), low-density lipoprotein receptor (LDLR) and transferrin receptor (Matter *et al.*, 1992), (Odorizzi and Trowbridge, 1997; Folsch *et al.*, 1999). One reason is that these cells lack the subunit μ1B of adaptor protein AP-1 (Folsch *et al.*, 2001). To check shrew-1 sorting in these cells, LLC-PK1 cells were plated on Transwell filters, transfected 24 h later with wild-type shrew-1-GFP, and allowed to achieve polarization for 5 d. After fixation, the cells were analyzed by confocal microscopy. Analysis of these cells revealed that wild-type shrew-1-GFP was localized predominantly at the apical plasma membrane (Figure 5A). However, we also observed that newly synthesized shrew-1-GFP also localized to the basolateral surface and was then distributed to the apical membrane (Figure 9, E and F). The shrew-1 mutant shrew-1-NTD5-GFP, also transiently transfected into LLC-PK1 cells, showed an apical steady-state distribution similar to that found for wild-type shrew-1 (Figure 5C).

We therefore tested whether introduction of μ1B of adaptor protein AP-1 into LLC-PK1 cells would restore sorting of wild-type shrew-1 to the basolateral membrane, but not of shrew-1-NTD5 lacking the cytoplasmic domain, because this truncation removes all basolateral sorting information, resulting in apical membrane sorting in MDCK cells (Figure 2D). For this purpose, LLC-PK1 cells were seeded on Transwell filters and cotransfected with either wild-type shrew-1-GFP and HA-tagged μ1B or with shrew-1-NTD5-GFP and μ1B. Five days after transfection, the cells were analyzed using confocal microscopy for cell surface appearance of shrew-1. As shown in Figure 5B, expression of μ1B-HA significantly enhanced the basolateral location of wild-type shrew-1. In contrast, shrew-1-NTD5 remained apical even after coexpression with μ1B-HA (Figure 5D).

Furthermore, we tested whether shrew-1 and μ1 subunits interact in LLC-PK1 cells by performing coimmunoprecipitation with anti-HA antibody. Western blots were then probed with GFP antibody. We could demonstrate that μ1B subunit formed a complex with shrew-1, whereas subunit μ1A did not. In addition, mutant shrew-1-NTD5 did not show any complex formation with μ1B (Figure 5F). In conclusion, μ1B subunit, which is incorporated into the AP-1B complex, is active in LLC-PK1 cells and recognizes signals for basolateral targeting within the cytoplasmic domain of shrew-1.

Double immunofluorescence microscopy experiments in MCF-7 cells transfected with shrew-1-GFP demonstrated colocalization of shrew-1-GFP with endogenous recycling endosome marker rab11 (Figure 6C). However, shrew-1-GFP displayed no colocalization with endogenous early endosome marker rab5 (Figure 6F).

Together, these data imply that the sorting of shrew-1 to the basolateral part of the membrane seems to require μ1B subunit and therefore probably AP-1B.

Use of Tannic Acid to Analyze Trafficking of Shrew-1 in Polarized MDCK Cells

Tannic acid is a fixative that disturbs the fusion of membrane vesicles derived from the TGN, or subsequent compartments, with the plasma membrane. Because tannic acid cannot pass through tight junctions it can be added selectively to either the apical or the basolateral side of polarized cells. This approach (Figure 7A) is rather useful for testing

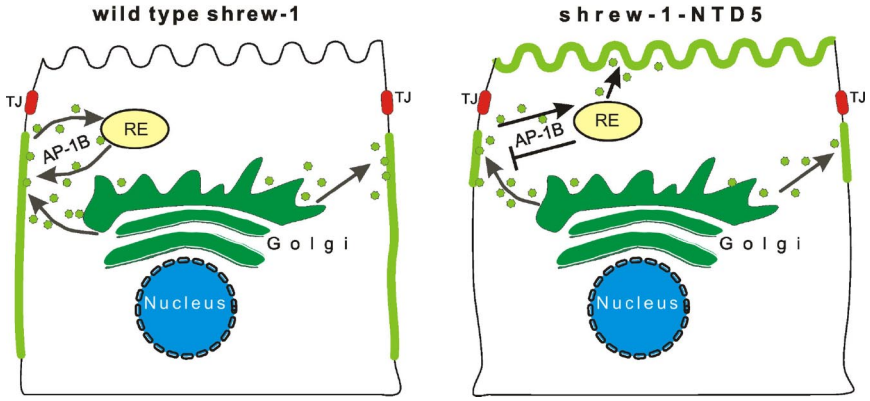

Figure 10. A sorting model suggested by the tannic acid experiments in Figure 6. Shrew-1-GFP (left) and shrew-1-NTD5-GFP (right) are similarly delivered to the basolateral membrane, and then recycled to the recycling endosome (RE). In contrast to wild type, shrew-1-NTD5-GFP cannot return to the basolateral membrane because it lacks the μ1B recognition motif and is therefore resorted to the apical membrane (left).

the order in which membrane proteins reach particular membrane domains (Polishchuk *et al.*, 2004).

We therefore used tannic acid treatment to dissect the route to the plasma membrane used by wild-type shrew-1 and the truncated cytoplasmic tail mutant shrew-1-NTD5 to the plasma membrane. This should help unravel whether the delivery of shrew-1 mutant follows directly to the apical membrane rather than passing through the basolateral membrane domain.

MDCK cells stably expressing wild-type shrew-1 or mutant shrew-1-NTD5 were plated on Transwell filters, propagated for 7 d, and then treated for 45 min with tannic acid added to either apical or basal growth medium. After fixation and staining of the tight junctions, the cells were analyzed by confocal microscopy, and the localization of shrew-1-GFP and shrew-1-NTD5-GFP was determined. We ensured the impermeability of confluent MDCK monolayers by measuring the electrical resistance before and after administration of tannic acid. In both cases, the electrical resistance was higher than 100 Ωcm^{-2}. Furthermore, to exclude membrane depolarization after treatment with tannic acid, we performed E-cadherin staining. The analysis of E-cadherin localization revealed that E-cadherin remained restricted to basolateral surface. Tannic acid administered to the apical medium resulted in normal basolateral distribution of wild-type shrew-1 (Figure 8C). The shrew-1 mutant previously localizing in the apical membrane could not longer be observed there, but in the lateral membrane and we could observe carrier accumulation close to the tight junction zone (Figure 7G). This suggested that the mutant shrew-1 was initially transported to the basolateral membrane and that subsequent protein resorting to the apical membrane was disrupted by tannic acid. Tannic acid added to the basal growth medium diminished the appearance of wild-type shrew-1 in the basolateral membrane. We observed protein accumulation near tight junctions, indicating that the Golgi-derived vesicles containing shrew-1 were unable to fuse with the plasma membrane (Figure 7D). Neither basolateral nor apical localization was observed when examining the shrew-1 mutant for polarized distribution after basal treatment with tannic acid (Figure 7H), but protein carriers accumulated in the proximity of tight junctions and the apical membrane domain.

The transient appearance of shrew-1-NTD5-GFP (Figure 8, F and G, x,z sections) in the basolateral membrane followed by accumulation at the apical surface suggested that shrew-1-NTD5-GFP reached the apical surface indirectly. Transcytosis was demonstrated by the fact that anti-shrew-1 antibody added to the basal medium was actively transported to the apical membrane and occurred there after 60 min (Figure 9, C and D).

This supports the idea that protein transport of mutant shrew-1-NTD5 showing apical steady-state distribution occurs via the basolateral membrane region (Figure 10).

DISCUSSION

Here, we show that the targeting of transmembrane protein shrew-1 to adherens junctions in polarized epithelial cells is mediated by signals contained in the cytoplasmic domain. Specifically, all three tyrosines therein are essential for basolateral targeting, because substituting each by alanine led to apical localization of shrew-1 in polarized MDCK cells. Similarly, substitution of leucine 303 by alanine or a dileucine motif by histidine and valine (LI396/397HV) also led to apical localization of shrew-1. The route of sorting most likely occurs through postendocytic mechanisms because mutant shrew-1 NTD5 (lacking the cytoplasmic domain), which normally targets to the apical membrane, occurred at the basolateral membrane in tannic acid-treated cells. Finally, adaptor protein AP-1B is required for the basolateral sorting of shrew-1, which forms a complex with AP-1B–specific subunit μ1B.

So far, the best characterized tyrosine-based protein sorting motifs are those with the consensus sequence YXXΦ, described as endosomal sorting signals for a number of transmembrane proteins (Bonifacino and Traub, 2003). Furthermore, there is evidence that a reversed motif YXXΦ, namely, ΦXXY, may also be an efficient functional sorting motif (Roush *et al.*, 1998). The latter occurs twice in shrew-1 as $FTAY_{350}$ and $VPVY_{368.}$ In line with this, a tyrosine-based motif, YXXΦ, inverted in the transferring receptor and in the LDL receptor reduced, but did not abolish internalization (Gironès *et al.*, 1991).

A sorting motif similar to YXXΦ is also present in shrew-1, but with a different number of residues between Y and Φ (YKSTF). Although structural studies have indicated that the spacing between Y and Φ is crucial for recognition by adaptor proteins (Owen and Evans, 1998), it seems that YXXXΦ can also be an efficient sorting signal, as supported by internalization studies of homomeric receptor P2X4 (Royle *et al.*, 2005). Thus, the number of amino acids between Y and Φ in tyrosine-based sorting motifs might not be as critical as previously postulated, and some variation in number and composition between residues Y and Φ is permitted.

Further analysis of shrew-1 cytoplasmic domain revealed that a single leucine (residue 303), but not the adjacent lysine (residue 304), is necessary for basolateral sorting. This is

reminiscent of a basolateral sorting motif in CD147 where mutation of the juxtamembrane leucine but not the adjacent lysine also leads to apical instead of basolateral localization in polarized MDCK cells (Deora *et al*., 2004). This suggests a strikingly similar basolateral targeting signal in both shrew-1 and CD147. Nevertheless, we cannot exclude that mutation L303A and the equivalent in CD147 might, for example, modulate the protein hydrophobicity in both cases, possibly affecting their secondary and tertiary structure, and thus influencing their trafficking in a nonspecific manner (discussed in Deora *et al*., 2004). In addition, accessibility of leucine residue 303 by an adaptor protein is difficult to imagine because it localizes close to the membrane.

Mutations of the leucines in the "acidic cluster dileucine" DXXLL of shrew-1 resulted in apical distribution in polarized MDCK cells. Such "acidic cluster dileucines," including a crucial aspartate 2 positions upstream have been described as recognition motifs for GGAs. These bind to, and hence are involved in, the sorting of cargo proteins from the TGN to endosomal compartments (Johnson and Kornfeld, 1992; Chen *et al*., 1997; Bonifacino, 2004). Furthermore, it is known that a dileucine motif in the C-terminal cytoplasmic domain of proteins is required for endocytosis (Bonifacino and Traub, 2003) and sometimes also for basolateral sorting (Bello *et al*., 2001; El Nemer *et al*., 1999). In contrast, another report postulates that dileucine motifs target proteins from the TGN to endosomal/lysosomal compartments (Sandoval and Bakke, 1994).

Evidently, the DXXLL motif is part of a potential casein kinase 2 phosphorylation site due to the presence of three serines before the aspartate. It has been shown that phosphorylation of serine residues upstream of the acidic dileucine signal results in tighter binding to the VHS domain of GGA adaptors (Kato *et al*., 2002). Thus, the presence of the three serines emphasizes the potential of this region for being a signal (Meggio *et al*., 1984; Boldyreff *et al*., 1994). Preliminary data from our laboratory suggesting serine phosphorylation of shrew-1 (our unpublished data) also support such an idea.

Interestingly, comparison of cytoplasmic amino acids between human, mouse, and zebrafish shrew-1 revealed a high degree of conservation (Figure 3B). In particular, the three tyrosines described above are conserved, including their positions. Zebrafish shrew-1 has an additional tyrosine at a position comparable with amino acid 360 in human and mouse. It remains to be seen whether this tyrosine is of functional importance for targeting in zebrafish. Also, the targeting motif DRHLI in human and mouse shrew-1 is almost identical in zebrafish, except this motif contains another negatively charged amino acid, glutamate, instead of aspartate (Figure 3B).

Together, the identification of several functionally and evolutionary conserved basolateral targeting signals in shrew-1 is rather unexpected. It is possible that the sum of all putative basolateral signals in the cytoplasmic tail of shrew-1 is necessary for proper routing to the target membrane, and, importantly, for retaining the protein there. Alternatively, it is conceivable that the different targeting signals provide distinct but overlapping functions.

MDCK cells use two different routes to target newly synthesized apically localized proteins to the apical surface: a direct route from the Golgi complex and an indirect or transcytotic route that involves an intermediate stop at the basolateral surface (Nelson and Yeaman, 2001). The mechanisms and proteins enabling transcytosis are generally unknown. Epithelial cell-specific sorting adaptor AP-1B, which is localized to recycling endosomes, plays a role in transcytotic or postendocyic sorting (Folsch *et al*., 1999; Gan *et al*., 2002) in MDCK cells (Traub and Apodaca, 2003). However, it has been shown for apically localized neuronglia cell adhesion molecule and vesicular stomatitis virus glycoprotein that these AP-1B–dependent cargo proteins are targeted from the TGN to the basolateral surface before endocytosis and then distributed to the apical surface (Ang *et al*., 2004; Polishchuk *et al*., 2004; Anderson *et al*., 2005). These findings suggest that AP-1B–dependent sorting, where AP-1B seems to function as a filter occurs in recycling endosomes (Ang *et al*., 2004) and that the recycling endosome plays an important role in polarized sorting in the endocytic pathway.

Two lines of evidence are in favor of the idea that targeting of shrew-1 is achieved via postendocytic sorting. First, routing of shrew-1-NTD5 (lacking the cytoplasmic domain) in the presence of tannic acid led to its accumulation at the basolateral surface, implying that it is initially attached to the basolateral membrane, and then redistributed to the apical membrane. This supports the view that wild-type shrew-1 is first delivered to the basolateral membrane where it is then retained by recognition of specific amino acid sequence motifs not present in mutant shrew-1-NTD5.

Additional evidence for postendocytic sorting was obtained by expressing wild-type shrew-1 and mutant shrew-1-NTD5 (cytoplasmic domain deletion) in LLC-PK1 cells lacking subunit μ1B of adaptor protein AP-1. In LLC-PK1 cells both wild-type and mutant shrew-1-NTD5 were predominantly found at the apical surface. This apical targeting could be reversed to basolateral targeting for shrew-1 wild type, but not for the mutant lacking basolateral sorting signals, by ectopic expression of μ1B. These results correlate with previous observations showing that AP-1B (containing subunit μ1B) prevents proteins (e.g., LDLR, which is delivered to the basolateral membrane) from switching to the apical membrane domain via postendocytic sorting mechanisms (Girotti and Banting, 1996; Gan *et al*., 2002).

In conclusion, our data provide evidence for a scenario (Figure 10) in which shrew-1 is primarily delivered to the basolateral membrane by a so far unknown mechanism. Once there, adaptor protein complex AP-1B is involved in retaining shrew-1 at the basolateral membrane. Sorting signals involved in this process may nevertheless differ from the signals involved in sorting at the TGN (Odorizzi and Trowbridge, 1997).

ACKNOWLEDGMENTS

We thank Avril Arthur-Goettig for critical reading of the manuscript and Heinz Schewe, Julija Raiz, and Monica Kamprad for experimental support. This work was supported by the Deutsche Forschungsgemeinschaft through Grant SFB 628, project P7.

REFERENCES

Anderson, E., Maday, S., Sfakianos, J., Hull, M., Winckler, B., Sheff, D., Folsch, H., and Mellman, I. (2005). Transcytosis of NgCAM in epithelial cells reflects differential signal recognition on the endocytic and secretory pathways. J. Cell Biol. *170*, 595–605.

Ang, A. L., Taguchi, T., Francis, S., Folsch, H., Murrells, L. J., Pypaert, M., Warren, G., and Mellman, I. (2004). Recycling endosomes can serve as intermediates during transport from the Golgi to the plasma membrane of MDCK cells. J. Cell Biol. *167*, 531–543.

Bello, V., Goding, J. W., Greengrass, V., Sali, A., Dubljevic, V., Lenoir, C., Trugnan, G., and Maurice, M. (2001). Characterization of a di-leucine-based signal in the cytoplasmic tail of the nucleotide-pyrophosphatase NPP1 that mediates basolateral targeting but not endocytosis. Mol. Biol. Cell *12*, 3004–3015.

Bharti, S., Handrow-Metzmacher, H., Zickenheiner, S., Zeitvogel, A., Baumann, R., and Starzinski-Powitz, A. (2004). Novel membrane protein shrew-1 targets to

cadherin-mediated junctions in polarized epithelial cells. Mol. Biol. Cell *15*, 397–406.

Boldyreff, B., Meggio, F., Pinna, L. A., and Issinger, O. G. (1994). Efficient autophosphorylation and phosphorylation of the beta-subunit by casein kinase-2 require the integrity of an acidic cluster 50 residues downstream from the phosphoacceptor site. J. Biol. Chem. *269*, 4827–4831.

Bonifacino, J. S. (2004). The GGA proteins: adaptors on the move. Nat. Rev. Mol. Cell Biol. *5*, 23–32.

Bonifacino, J. S., and Dell'Angelica, E. C. (1999). Molecular bases for the recognition of tyrosine-based sorting signals. J. Cell Biol. *145*, 923–926.

Bonifacino, J. S., and Traub, L. M. (2003). Signals for sorting of transmembrane proteins to endosomes and lysosomes. Annu. Rev. Biochem. *72*, 395–447.

Brown, A., Muth, T., and Caplan, M. (2004). The COOH-terminal tail of the GAT-2 GABA transporter contains a novel motif that plays a role in basolateral targeting. Am. J. Physiol. *286*, C1071–C1077.

Chen, H. J., Yuan, J., and Lobel, P. (1997). Systematic mutational analysis of the cation-independent mannose 6-phosphate/insulin-like growth factor II receptor cytoplasmic domain. An acidic cluster containing a key aspartate is important for function in lysosomal enzyme sorting. J. Biol. Chem. *272*, 7003–7012.

Deora, A. A., Gravotta, D., Kreitzer, G., Hu, J., Bok, D., and Rodriguez-Boulan, E. (2004). The basolateral targeting signal of CD147 (EMMPRIN) consists of a single leucine and is not recognized by retinal pigment epithelium. Mol. Biol. Cell *15*, 4148–4165.

Duffield, A., Folsch, H., Mellman, I., and Caplan, M. J. (2004). Sorting of H,K-ATPase beta-subunit in MDCK and LLC-PK cells is independent of mu 1B adaptin expression. Traffic *5*, 449–461.

El Nemer, W., Colin, Y., Bauvy, C., Codogno, P., Fraser, R. H., Cartron, J. P., and Le Van Kim, C. L. (1999). Isoforms of the Lutheran/basal cell adhesion molecule glycoprotein are differentially delivered in polarized epithelial cells. Mapping of the basolateral sorting signal to a cytoplasmic di-leucine motif. J. Biol. Chem. *274*, 31903–31908.

Folsch, H., Ohno, H., Bonifacino, J. S., and Mellman, I. (1999). A novel clathrin adaptor complex mediates basolateral targeting in polarized epithelial cells. Cell *99*, 189–198.

Folsch, H., Pypaert, M., Schu, P., and Mellman, I. (2001). Distribution and function of AP-1 clathrin adaptor complexes in polarized epithelial cells. J. Cell Biol. *152*, 595–606.

Gan, Y., McGraw, T. E., and Rodriguez-Boulan, E. (2002). The epithelial-specific adaptor AP1B mediates post-endocytic recycling to the basolateral membrane. Nat. Cell Biol. *4*, 605–609.

Gironès, N., Alverez, E., Seth, A., Lin, I. M., Latour, D. A., and Davis, R. J. (1991). Mutational analysis of the cytoplasmic tail of the human transferrin receptor. Identification of a sub-domain that is required for rapid endocytosis. J. Biol. Chem. *266*, 19006–19012.

Girotti, M., and Banting, G. (1996). TGN38-green fluorescent protein hybrid proteins expressed in stably transfected eukaryotic cells provide a tool for the real-time, in vivo study of membrane traffic pathways and suggest a possible role for ratTGN38. J. Cell Sci. *109*, 2915–2926.

Hirst, J., and Robinson, M. S. (1998). Clathrin and adaptors. Biochim. Biophys. Acta *1404*, 173–193.

Ikonen, E., and Simons, K. (1998). Protein and lipid sorting from the trans-Golgi network to the plasma membrane in polarized cells. Semin. Cell Dev. Biol. *9*, 503–509.

Johnson, K. F., and Kornfeld, S. (1992). The cytoplasmic tail of the mannose 6-phosphate/insulin-like growth factor-II receptor has two signals for lysosomal enzyme sorting in the Golgi. J. Cell Biol. *119*, 249–257.

Kato, Y., Misra, S., Puertollano, R., Hurley, J. H., and Bonifacino, J. S. (2002). Phosphoregulation of sorting signal-VHS domain interactions by a direct electrostatic mechanism. Nat. Struct. Biol. *9*, 532–536.

Kirchhausen, T. (1999). Adaptors for clathrin-mediated traffic. Annu. Rev. Cell Dev. Biol. *15*, 705–732.

Kirchhausen, T. (2000). Three ways to make a vesicle. Nat. Rev. Mol. Cell Biol. *1*, 187–198.

Matter, K. (2000). Epithelial polarity: sorting out the sorters. Curr. Biol. *10*, R39–R42.

Matter, K., Hunziker, W., and Mellman, I. (1992). Basolateral sorting of LDL receptor in MDCK cells: the cytoplasmic domain contains two tyrosine-dependent targeting determinants. Cell *71*, 741–753.

Meggio, F., Marchiori, F., Borin, G., Chessa, G., and Pinna, L. A. (1984). Synthetic peptides including acidic clusters as substrates and inhibitors of rat liver casein kinase TS (type-2). J. Biol. Chem. *259*, 14576–14579.

Mellman, I. (1993). Endocytosis and the entry of intracellular parasites. Infect. Agents Dis. *2*, 186–192.

Mostov, K., Su, T., and ter Beest, M. (2003). Polarized epithelial membrane traffic: conservation and plasticity. Nat. Cell Biol. *5*, 287–293.

Mostov, K. E., Verges, M., and Altschuler, Y. (2000). Membrane traffic in polarized epithelial cells. Curr. Opin. Cell Biol. *12*, 483–490.

Nelson, W. J. (2003). Adaptation of core mechanisms to generate cell polarity. Nature *422*, 766–774.

Nelson, W. J., and Yeaman, C. (2001). Protein trafficking in the exocytic pathway of polarized epithelial cells. Trends Cell Biol. *11*, 483–486.

Odorizzi, G., and Trowbridge, I. S. (1997). Structural requirements for basolateral sorting of the human transferrin receptor in the biosynthetic and endocytic pathways of Madin-Darby canine kidney cells. J. Cell Biol. *137*, 1255–1264.

Orsel, J. G., Sincock, P. M., Krise, J. P., and Pfeffer, S. R. (2000). Recognition of the 300-kDa mannose 6-phosphate receptor cytoplasmic domain by 47-kDa tail-interacting protein. Proc. Natl. Acad. Sci. USA *97*, 9047–9051.

Owen, D. J., and Evans, P. R. (1998). A structural explanation for the recognition of tyrosine-based endocytotic signals. Science *282*, 1327–1332.

Pearse, B. M., and Robinson, M. S. (1990). Clathrin, adaptors, and sorting. Annu. Rev. Cell Biol. *6*, 151–171.

Polishchuk, R., Di Pentima, A., and Lippincott-Schwartz, J. (2004). Delivery of raft-associated, GPI-anchored proteins to the apical surface of polarized MDCK cells by a transcytotic pathway. Nat. Cell Biol. *6*, 297–307.

Rodriguez-Boulan, E., and Nelson, W. J. (1989). Morphogenesis of the polarized epithelial cell phenotype. Science *245*, 718–725.

Roush, D. L., Gottardi, C. J., Naim, H. Y., Roth, M. G., and Caplan, M. J. (1998). Tyrosine-based membrane protein sorting signals are differentially interpreted by polarized Madin-Darby canine kidney and LLC-PK1 epithelial cells. J. Biol. Chem. *273*, 26862–26869.

Royle, S. J., Qureshi, O. S., Bobanovic, L. K., Evans, P. R., Owen, D. J., and Murrell-Lagnado, R. D. (2005). Non-canonical YXXGPhi endocytic motifs: recognition by AP2 and preferential utilization in P2X4 receptors. J. Cell Sci. *118*, 3073–3080.

Sandoval, I. V., and Bakke, O. (1994). Targeting of membrane proteins to endosomes and lysosomes. Trends Cell Biol. *4*, 292–297.

Slepnev, V. I., and De Camilli, P. (2000). Accessory factors in clathrin-dependent synaptic vesicle endocytosis. Nat. Rev. Neurosci. *1*, 161–172.

Traub, L. M., and Apodaca, G. (2003). AP-1B: polarized sorting at the endosome. Nat. Cell Biol. *5*, 1045–1047.

Yeaman, C., Grindstaff, K. K., and Nelson, W. J. (1999). New perspectives on mechanisms involved in generating epithelial cell polarity. Physiol. Rev. *79*, 73–98.